WILEY

Prospects and challenges of mini-LED and micro-LED displays

Yuge Huang SID Student Member[1] | Guanjun Tan SID Student Member[1] | Fangwang Gou SID Student Member[1] | Ming-Chun Li[2] | Seok-Lyul Lee SID Fellow[2] | Shin-Tson Wu SID Fellow[1] (iD)

[1] College of Optics and Photonics, University of Central Florida, Orlando, Florida

[2] AU Optronics Corp., Hsinchu, Taiwan

Correspondence
Shin-Tson Wu, College of Optics and Photonics, University of Central Florida, Orlando, Florida 32816, USA.
Email: swu@ucf.edu

Funding information
a.u.Vista, Inc.

Abstract

We review the emerging mini/micro–light-emitting diode (LED) displays featuring high dynamic range and good sunlight readability. For mini-LED backlit liquid crystal displays (LCDs), we quantitatively evaluate how the device contrast ratio, local dimming zone number, and local light profile affect the image quality. For the emissive mini/micro-LED displays, the challenges of ambient contrast ratio and size-dependent power efficiency are analyzed. Two figure-of-merits are proposed for optimizing the optical and electrical performances of mini/micro-LED displays.

KEYWORDS
ambient contrast ratio, halo effect, high-dynamic range, internal quantum efficiency, local dimming, mini/micro-LED, size effect, sunlight readability

1 | INTRODUCTION

Presently, liquid crystal display (LCD)[1] and organic light-emitting diode (OLED) display[2] are two dominating technologies for smartphones, pads, monitors, and TVs. Each technology has its own pros and cons.[3] For example, LCD's major advantages are long lifetime, high peak brightness, and low cost, while OLED's distinctive features are true black state[4] and ultrathin profile, which enables flexible displays. They are comparable in color gamut,[5] resolution, motion picture response time,[6] and power consumption. However, LCD has two shortcomings to overcome: limited contrast ratio (CR ~ 1000-5000:1) and flexibility. On the other hand, OLED's major challenges are compromised lifetime as luminance increases[7,8] and relatively higher cost. In order to faithfully reproduce nature scenes, high dynamic range (HDR) is critically important.[9] To achieve HDR, a display device should have high peak luminance (L_p > 1000 cd/m^2) and excellent dark state (less than 0.01 cd/m^2). LCD has the former

characteristic but lacks the latter, while OLED is opposite. Both LCD and OLED camps are working hard to improve their own drawbacks.

Recently, mini-LED and micro-LED displays[10–12] are attracting extensive attentions for their HDR,[13] high ambient CR (ACR),[14] thin profile, and low power consumption.[12,15–17] When a mini-LED array is employed as LCD backlight, the local dimming technology[15,16,18–24] could boost the panel's CR[25] to 1 000 000:1. When mini/micro-LED chips are integrated in self-emissive displays, ie, without LCD panel, it presents an excellent dark state as well as several times higher peak luminance than LCDs and OLED displays.[12,26] Moreover, their simple structure, freeform shape factor, high aperture ratio, wide viewing angle, and wide operation temperature range could make these displays ubiquitous for indoor and outdoor applications.[26,27]

In this paper, we will first introduce mini/micro-LED displays, emphasizing on their common challenges and potential solutions. In Section 2, we will present mini-LED backlit LCD beginning from optical system

structure, followed by common issues of local dimming—halo effect and clipping effect—and finally some proposed solutions. A simplified simulation model is utilized to evaluate the quantitative contribution of each design factor. In Section 3, we will discuss mini/micro-LED as emissive displays. In this category, two approaches can be considered for achieving full colors: (1) color conversion, such as using blue LED to pump green and red phosphors or quantum dots,[28–31] and (2) RGB LED chips.[32,33] The former has been reviewed recently,[34] while for the latter, we will analyze two important issues: internal reflection and chip size dependent internal quantum efficiency (IQE). A quantitative system evaluation method will be proposed, followed by exemplary optimization suggesting the best device structure and LED chip size. Although the high-yield mass production of small-chip micro-LED (less than 50 μm) is still under active development, the fabrication of mini-LED with larger chip size (100-500 μm) is relatively mature so that commercial panels are stepping into market at a reasonable price. Our work would provide useful guidelines for system design optimizations of mini/micro-LED displays.

2 | MINI-LED BACKLIT LCDS

2.1 | Mini-LED backlit LCD system

Conventional LCDs suffer from a relatively low CR, and some possible causes are nonuniform alignment of the liquid crystal (LC) layer, scattering of the color filters (CFs), and diffraction from the pixelated electrodes.[35] To boost CR, *local dimming* with spatially segmented backlight unit (BLU) is an effective approach. Each segment, the so-called local dimming zone, is controlled independently. With 10-bit backlight modulation, the CR can increase from 1000 to 5000:1 to approximately 1 000 000:1. A schematic mini-LED backlit LCD is shown in Figure 1. For discussion purpose, let us assume each mini-LED has a square shape. The emitted light propagates a distance (eg, adhesive layer) before reaching the diffuser. The distance and scattering strength of the diffuser need to be optimized so that the outgoing light is spatially uniform before entering the LC layer.
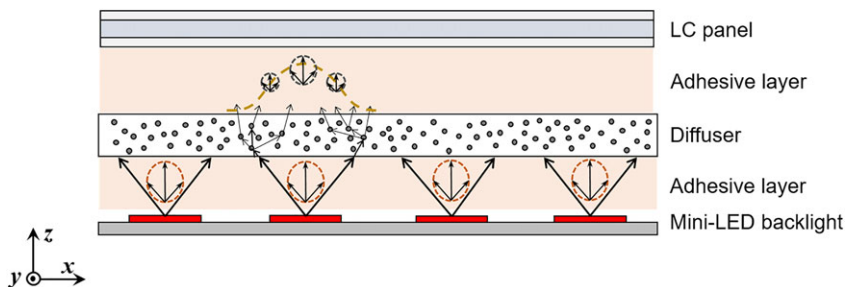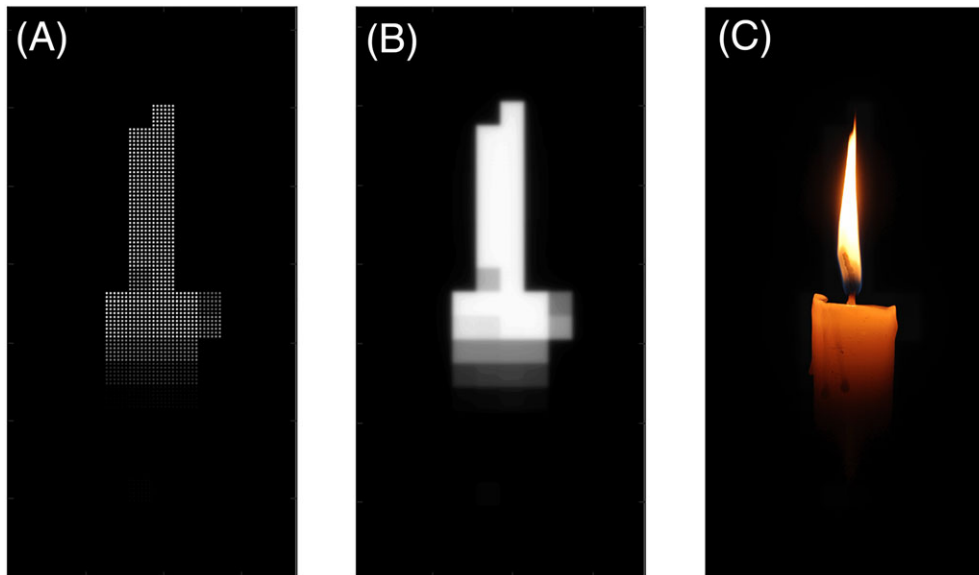
Next, we use an exemplary candle picture as shown in Figure 2 to illustrate the light modulation process of mini-LED backlit LCDs. Here, the backlight consists of 12 × 24 local dimming zones and each zone contains 6 × 6 mini-LEDs in order to achieve a desired luminance. According to the image content, the mini-LEDs in each dimming zone are predetermined to show different gray levels, as Figure 2A depicts. After passing through the diffuser, the outgoing light spreads out uniformly before reaching the LCD panel (Figure 2B). The gray level of each LCD pixel is controlled by a thin-film-transistor (TFT), and each CF only transmits the designated color. Finally, a full-color image as Figure 2C is generated.

2.2 | Challenges of local dimming LCDs

Mini-LED BLU enables a new LCD with high peak luminance, HDR, and thin form factor,[26] and in the meantime suppressing the undesired halo effect and clipping effect. Conventional edge-lit LCDs[15,16] feature thin profile, but the light guide plate is relatively thick if a high-luminance large-area LED array is adopted. On the other hand, conventional direct-lit LCDs with fewer number of LEDs[20,22] can provide high luminance and HDR, but a relatively long travel distance is needed to ensure good backlight uniformity. In comparison, the small chip size and large number of mini-LEDs make the light to spread out evenly so that the required optical distance between LED and diffuser is shorter.

Halo effect and clipping effect are common issues in local dimming LCDs. Halo effect is the light leakage from bright objects to adjacent dark areas. Clipping effect comes from the insufficient luminance in a local dimming zone when the adjacent zones are dimmed. Figure 3 schematically shows these two effects. The center of the local dimming zones are $x_{zone} = 0, \pm 1, \pm 2, ...$ with interval $\Delta x_{zone} = 1$. In Figure 3, only the center zone at $x_{zone} = 0$ is at peak luminance while the surrounding zones are dimmed. Ideally, the luminance of each zone should be uniform and independently controlled, as Figure 3A shows. However, in practice, the intensity of each local dimming zone is contributed by not only the

FIGURE 1 Schematic diagram of mini–light-emitting diode (LED) backlit liquid crystal display (LCD)

FIGURE 2 Light modulation of mini–light-emitting diode (LED) backlit liquid crystal display (LCD): A, mini-LED backlight modulation; B, luminance distribution of the light incident on the liquid crystal (LC) layer; and C, displayed image after LCD modulation
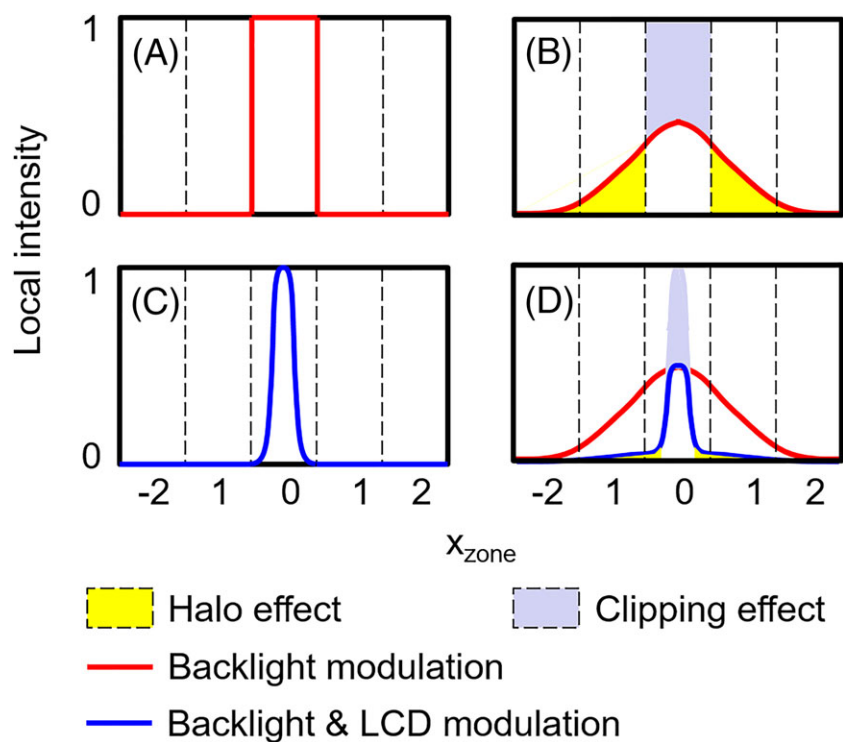
FIGURE 3 Schematic show of halo effect and clipping effect in local dimming liquid crystal displays (LCDs): A, ideal and B, practically obtainable local dimming intensity profiles; C, target intensity profile after LCD modulation; D, practically obtainable intensity profile with halo effect and clipping effect

aligned light source but also the light leakage from adjacent zones, as Figure 3B depicts. As a result, the intensity in the center zone is "clipped" to one half (purple area), and the light leaks to adjacent zones forming "halo" (yellow area). Afterward, a LCD panel modulates the light from the BLU (red lines) to get finer details (blue lines). While the target light profile is plotted in Figure 3C, the displayed image quality could be degraded as Figure 3D shows.

A variety of local dimming algorithms have been developed to suppress these two effects, from the basic "maximum," "average" methods, to the complex point spreading function (PSF) integrations.[19,21,23] In 2013, Burini et al compared different algorithms and conducted optimization to find the best trade-off point between halo and clipping effects with power constraint.[24]

From the hardware aspect, an infinitely high CR or pixel-level dimming could eliminate these two effects. In

a practical HDR LCD design, increasing the number of local dimming zones could reduce the dark area affected by halo effect (the yellow area in Figure 3B), while a higher LCD CR can effectively suppress the halo effect in the bright zones (the little light leakage in the central zone as indicated by the yellow area in Figure 3D). Methods for reducing zone crosstalk is helpful to mitigate both halo effect and clipping effect. In the following part, we will demonstrate why mini-LED BLU is promising to function as a highly independent local dimming controller.

2.3 | Mini-LED BLU solutions

The system configuration of mini-LED backlit LCD determines the severity of halo effect and clipping effect and affects the total thickness of BLU. The number of local dimming zones and LCD's CR have the dominant impacts on local dimming effect. However, between two comparable panels, sometimes the one with fewer local dimming zones could exhibit a better performance, which is contradictory to the general trend. This conflict comes from the different optical designs, where LED light expansion and local light confinement also jointly contribute to the final local dimming performance. In the following, we will discuss the influence of each factor and then suggest the corresponding optimization strategies. The following discussions are based on a 6.4-inch smartphone placed at 25-cm viewing distance, but these results can be scaled up and applied to large-size panels as well.

2.3.1 | Number of local dimming zones and LCD CR

In 2018, Tan et al demonstrated that mini-LED BLU could effectively suppress halo effect if the LCD CR and the density of local dimming zones are properly chosen.[13] By simulating the displayed images of a mini-LED backlit LCD with different system configurations and conducting subjective experiments, they found the peak signal-to-noise ratio in the CIE 1976 $L*a*b*$ color space (LabPSNR) can be used as a metric to evaluate the halo effect. When LabPSNR > 47.7 dB, only less than 5% people could differentiate the displayed image on a mini-LED backlit LCD from the original picture.

Figure 4 shows the correlation between the LCD CR and local dimming zone number. The black dashed lines represent that the halo effect is unnoticeable. From Figure 4, we find that approximately 3000 local dimming zones is required for a fringing-field switching (FFS) LCD with CR = 2000:1, and approximately 200 zones are
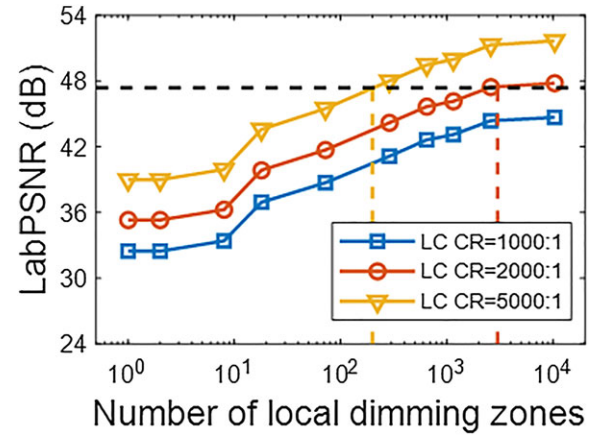
FIGURE 4 Simulated LabPSNR for high-dynamic range (HDR) display systems with various local dimming zone numbers and contrast ratio

required for a multidomain vertical alignment (MVA) LCD with CR = 5000:1. However, if an LCD's CR is lower than 1000:1, then even 10 000 zones is still inadequate.

2.3.2 | LED light expansion

From mini-LED BLU to LC layer, the light profile of each LED could expand from the original square-shaped Lambertian distribution to a Gaussian-like profile. The final profile can be influenced by several factors including the LED emission aperture, the distance between mini-LEDs and diffuser, and other optical layers such as brightness enhancement film (BEF). Figure 5 depicts an exemplary one-dimensional light profile. Here, we assume there are six mini-LEDs ($N_{LED} = 6$) located at $x_{LED} = \pm0.5, \pm1.5$, and ±2.5, with an interval $\Delta x_{LED} = 1$. In reality, there are 6×6 mini-LEDs in the central dimming zone. They are turned-on together, while the adjacent zones are dimmed to the dark state. In Figure 5, each black curve depicts the light profile entering the LC layer from each individual mini-LED, and the blue curves delineate the single-zone light profile. Because the light experiences propagation and diffusion before entering the LC layer, here, we use Gaussian function to fit the expanded single-LED light profile:

$$I(x_{LED}) \propto \exp\left[-\frac{(x_{LED}-x_{LED\_c})^2}{2\sigma^2}\right], \quad (1)$$

where x_{LED_c} is the locus of the source LED, and σ is an expansion characteristic parameter.

In Figure 5, the vertical red dashed lines denote the local dimming zone borders. As we can see, a small σ/x_{LED} helps confine the light in the local area (Figure 5A) while more than one-half of the light energy would spread outside
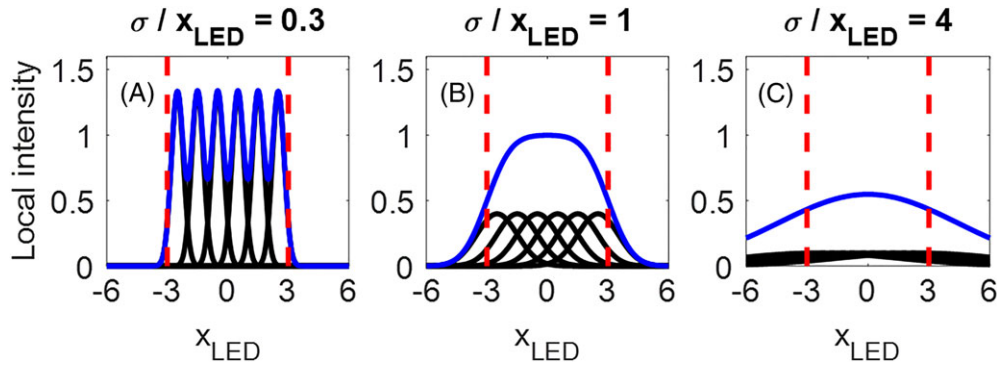
FIGURE 5 Simulated spatial profiles of local dimming backlight units (BLUs) with different σ/x_{LED} values

the zone when σ/x_{LED} is large (Figure 5C). Such a crosstalk could impair the local dimming function and give rise to the unwanted halo effect and clipping effect.

Figure 6 shows that for a given number of LEDs in a local dimming zone (N_{LED}), better image fidelity (higher LabPSNR) can be obtained by a smaller σ/x_{LED}, corresponding to a smaller LED emission aperture and shorter optical distance. The latter leads to a thinner panel profile. However, the associated challenges are thermal management, manufacturing yield, and especially the compromised luminous uniformity. Figure 5A shows that if the LED light does not spread wide enough, the resultant backlight intensity could be very sensitive to the spatial location. Therefore, a proper σ/x_{LED} should be selected. For instance, $\sigma/x_{LED} = 0.5$ could provide greater than 97% backlight uniformity, which enables unnoticeable halo effect on a local dimming LCD with 2×2 LEDs per local dimming zone and CR = 2000:1 (Figure 6B). In Figure 6A to 6C, if we compare the LabPSNR values at $\sigma/x_{LED} = 0.5$ and an identical CR, we find that a smaller N_{LED} leads to a higher LabPSNR. The reason is that, here, we use the same LED dimension parameters and panel size for simulation. In other words, the smaller N_{LED}, the larger number of local dimming zones, therefore the higher LabPSNR. In a mini-LED backlit LCD system, σ/x_{LED} can be obtained by Gaussian fitting the expanded spatial luminous profile of a single mini-LED.

### 2.3.3 | Local light confinement

To reduce crosstalk between adjacent local dimming zones without compromising uniformity, optical structures such as bank isolation[36] or lens collimation[37] can be employed in a period of zone pitch (p_{zone}). Ideally, a rectangular light profile can generate uniform local dimming backlight without crosstalk. Whereas in practical designs, only flattop profile can be realized, which can be described by a super-Gaussian function as

$$I(x_{zone}) \propto \exp\left[-\left|\frac{x_{zone}-x_{zone\_c}}{\sigma}\right|^{\beta}\right]. \quad (2)$$

Similar to above discussion, here, we assume the center of the local dimming zones (x_{zone_c}) are $x_{zone} = 0$, ±1, ±2, ... with interval $\Delta x_{zone} = 1$. In Figure 7, each black curve depicts a spatial profile of light generated by the zone under its curve center, while the red dashed lines delineate the borders of the zone at $x_{zone\_c} = 0$. We set $\sigma/x_{zone} \sim 0.5$ in order to obtain good overall uniformity, as the blue curves indicate. Figure 7A to 7C shows that as β increases from 2 to 25, the crosstalk is reduced so that the clipping effect is lessened accordingly. Although the uniformity is improved noticeably from Figure 7A to 7C, the abrupt luminance change at zone borders is still observable (Figure 7C) at a large β. If the compensation
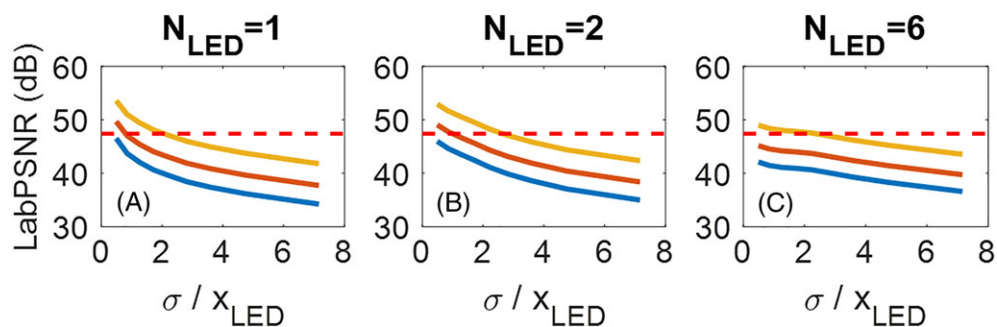
FIGURE 6 Simulated LabPSNR for high-dynamic range (HDR) display systems with different N_{LED}. The blue, red, and yellow lines stand for contrast ratio (CR) = 1000:1, 2000:1, and 5000:1, respectively
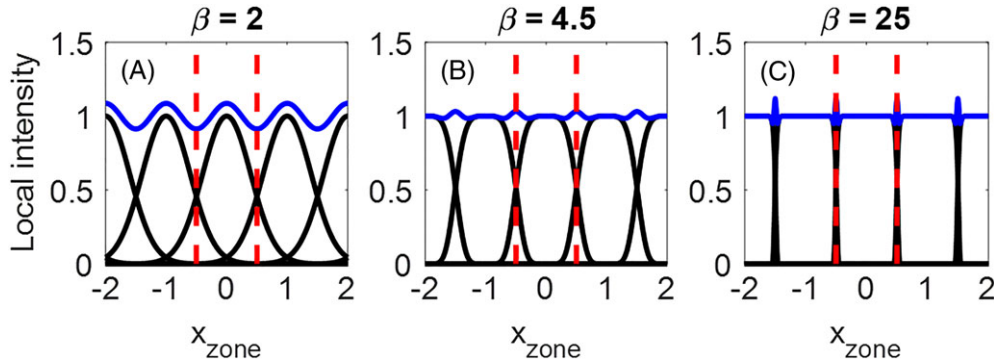
FIGURE 7 Simulated spatial profiles of different local dimming backlight unit (BLU) with different β

at borders is not performed carefully, the incongruous lines may be noticeable in the actual display panel. In practical manufacturing, uneven distribution of local dimming zone and misalignment between dimming zone and compensation may aggravate this issue.

Figure 8 demonstrates that good light confinement (high β) helps improve image quality. As β increases, LabPSNR increases initially but saturates as β exceeds 4.5. This implies local light confinement is helpful to certain degree. In contrast, high CR and short p_{zone} help enhance the LabPSNR value more obviously. When $\beta > 2$, an unnoticeable halo effect can be achieved for the LCDs with CR > 1000:1 (blue lines), 2000:1 (red lines), and 5000:1 (yellow lines) with $p_{zone} = 1$ mm (Figure 8A), 2 mm (Figure 8B), and 6 mm (Figure 8C), respectively. In practice, β can be extracted from a mini-LED enhanced LCD by super-Gaussian fitting the spatial luminous profile of single-lit local dimming zone.

3 | MINI/MICRO-LED EMISSIVE DISPLAYS

In Section 2, we discussed strategies to achieve HDR display with mini-LED enhanced local dimming LCDs. From here on, we will introduce mini/micro-LED as emissive displays: each LED chip serves as a color pixel

without any LCD panel. Presently, the major technical challenges are in three aspects: fabrication yield and cost due to mass transfer, ACR due to strong internal reflection, and decreased IQE as the chip size decreases. The high cost is associated with the relatively low fabrication yield.[38] Defects could be generated by LED chips, particles, and the complex massive transfer procedure.[27,39] To ensure display quality, color uniformity should be strictly controlled over the whole panel through multiple transfers.[32] Taking a 4K full-color display as an example, if the process yield is 99.99%, then there are approximately 2200 bad subpixels to be repaired. A yield as high as 99.9999% is required in order to reduce the number of bad subpixels to approximately 22 counts. Ideally, a good display should be defect-free. In order to improve yield and accelerate production speed, a two-step mass transfer approach has been developed.[33] In the first step, "good" mini/micro-LEDs are transferred from epitaxial wafers to an interposer substrate or cartridge array. After that, the patterned LEDs are transferred to display substrate.[38] From the cost management viewpoint, small LED chip size is preferred. The *estimated* die cost of Samsung's 146-inch 4K micro-LED TV "The Wall" by Yole Development is approximately $30 000, making the price unaffordable for average consumers. Similar to other technologies, the initial high cost could be reduced dramatically as the manufacturing technique becomes
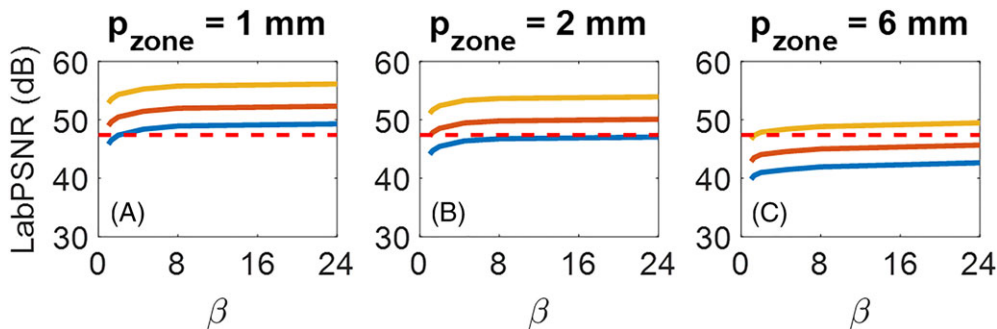
FIGURE 8 Simulated LabPSNR for high-dynamic range (HDR) display systems with various p_{zone}. The blue, red, and yellow lines stand for liquid crystal display's (LCD's) contrast ratio (CR) = 1000:1, 2000:1, and 5000:1, respectively

mature. However, device structure should be optimized beforehand. In the following sections, we will discuss some design strategies by analyzing the optical (eg, ACR) and electrical (eg, IQE) performances in detail.

3.1 | Ambient CR

The CR of a display device is usually measured at dark ambient. In the presence of ambient light, the CR could be deteriorated dramatically because of the surface and interface reflections. Under such a circumstance, ACR is a more meaningful metric to compare because it is what the viewer actually experiences.[14] The ACR can be expressed as follows:

$$ACR = \frac{L_{on} + \frac{I_{am}}{\pi} \cdot R_L}{L_{off} + \frac{I_{am}}{\pi} \cdot R_L}. \quad (3)$$

Assuming luminous reflectance $R_L = 4\%$ and CR $\approx 10^6{:}1$ (off-state luminance $L_{off} \approx 0$), we simulate the images with different display on-state luminance (L_{on}) and ambient light illuminance (I_{am}). Results are summarized in Figure 9. At a given peak luminance, as the environment light gets stronger (I_{am} increases), ACR decreases and the displayed image is gradually washed out. To improve the ACR of an LCD, a straightforward way is to boost the display luminance, say from 1000 to 2500 cd/m². However, the light leakage in dark state also increases, resulting in a limited ACR.

3.1.1 | ACR calculation and metric of optical performance

Figure 10 depicts the device structure of an RGB mini/micro-LED emissive display, in which the LED array is encapsulated by bonding layers and a protection glass. For this device structure, the luminous reflectance (R_L) can be described by

$$R_L = R_{ex} + R_{in} = R_s + AP \cdot (1 - R_s) \cdot R_{L\_LED} \cdot T. \quad (4)$$

In Figure 10 and Equation 4, R_s, AP, and R_{L_LED} stand for surface reflectance, aperture ratio, LED luminous reflectance, respectively, and T represents the transmittance of the reflected ambient light from LED through additional optical components, such as CF and circular polarizer (CP). In each pixel, the RGB LED chips only occupy a portion of the pixel, and the rest area is covered by black matrix (BM); as a result, the AP is usually small. In Equation 4, R_L consists of two terms: external reflection (R_{ex}) at the air-glass interface and internal reflection (R_{in}) by LEDs, as illustrated by the red arrows and cyan arrows in Figure 10, respectively. To reduce R_L, BM, CF, and CP are helpful to reduce R_{in}, while antireflection (AR) surface treatment helps reduce R_{ex}.

From the layout of two pixels depicted in Figure 11, the aperture ratio and characteristic LED chip size (s) are defined as

$$AP = \frac{\text{emission area}}{\text{whole area}} = \frac{3s^2}{p^2}; \quad (5)$$

Ambient illuminance (lux)		Display peak luminance (cd/m²)		
		625	1000	2500
Indoor lighting	200	250:1	400:1	1000:1
Cloudy day	2000	25:1	40:1	100:1
Full daylight	20,000	3.5:1	4.9:1	10.8:1
Direct sunlight	100,000	1.5:1	1.8:1	3.0:1

FIGURE 9 Simulated displayed images with different peak luminance and ambient illuminance. The ambient contrast ratio (ACR) is marked on the right bottom corner of each picture
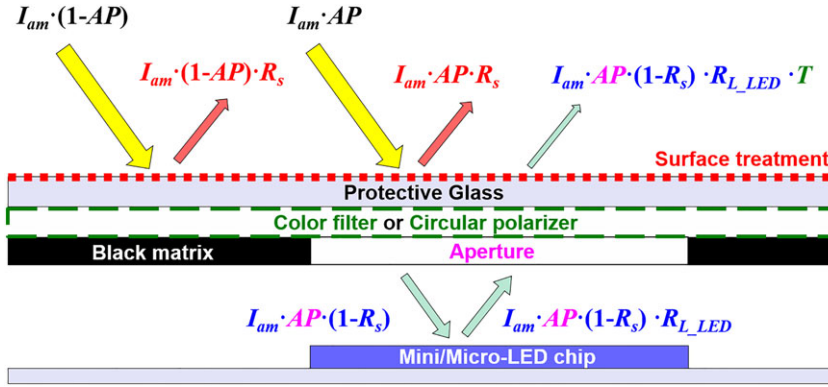
FIGURE 10 Scheme demonstration of ambient light reflection on mini/micro–light-emitting diode (LED) emissive display panels. Red arrows and cyan arrows correspond to external reflection and internal reflection, respectively
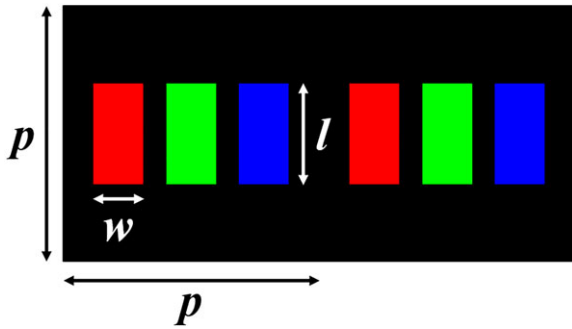
FIGURE 11 Pixel layout and dimensions of a mini/micro–light-emitting diode (LED) display. Each color pixel consists of three R/G/B subpixels

$$s = \sqrt{w \cdot l}. \tag{6}$$

Here, w and l denote the width and length of a single LED chip, respectively, and p stands for the pixel pitch length. Because BM absorbs the incident ambient light, only the light falls on the aperture would be internally reflected. This explains why the R_{in} term is related to AP in Equation 4.

The optical structure influences R_L and the on-state display luminance L_{on}. For easier comparison, we define a display luminance coefficient α with $L_{on} = \alpha \cdot L_0$ and a LED reflectance coefficient β by $R_{L\_LED} = \beta \cdot R_0$. Here, L_0 and R_0, respectively, stand for the on-state luminance and LED luminous reflectance of the benchmark structure: mini/micro-LED with indium tin oxide (ITO) electrode, well-aligned BM, and without any additional optical element, such as CF or CP. When we replace the bottom electrode from ITO to another material, the display luminance could be boosted by α times, while the LED reflectance is changed by β times. These effective coefficients are the properties of electrode materials and should be obtained through simulations or experiments. For an emissive mini/micro-LED display, the ideal off-state display luminance L_{off} should be zero. But in reality, it may have a small crosstalk-induced light leakage. Here, we assume the display has a high intrinsic CR = L_{on}/L_{off} > 1 000 000:1 and L_{off} << $(I_{am}/\pi) \cdot R_L$. To ensure a reasonably good sunlight readability, we also assume ACR >> 1. Under such conditions, Equation 3 can be approximated as

$$ACR \approx \frac{\alpha \cdot L_0 + \dfrac{I_{am}}{\pi} \cdot R_L}{\dfrac{I_{am}}{\pi} \cdot R_L} = 1 + \frac{\pi \cdot L_0}{I_{am}} \cdot \frac{\alpha}{R_L} \approx \frac{\pi \cdot L_0}{I_{am}} \cdot \frac{\alpha}{R_L}, \tag{7}$$

where

$$R_L = R_s + AP \cdot (1 - R_s) \cdot \beta \cdot R_0 \cdot T. \tag{8}$$

Equation 7 suggests a quantitative metric to evaluate the optical performance of a mini/micro-LED emissive display system. The first term $\pi \cdot L_0/I_{am}$ represents the ratio of intrinsic display luminance to ambient luminance, which depends on the applied LED current and the ambient condition. Differently, the second term α/R_L originates from display optics. Therefore, we call it as the figure-of-merit of optical design (FoM_o):

$$FoM_o = \frac{\alpha}{R_L}. \tag{9}$$

The influence of the optics part is governed by the numerical coefficients in Equations 8 and 9, such as α, β, T, R_s, and AP. In the following sections, we will analyze how each optical component affects the ACR.

3.1.2 | LED electrode

The bottom electrode of LED affects the light emission efficiency. Besides ITO, multilayer metal electrode can also be used for LEDs to achieve good ohmic contact. A typical structure for forming multilayer metal contact contains three parts[40]: (1) a thin layer physically attached to the semiconductor to form good ohmic contact, eg, a thin ITO[41]; (2) intermediate layers serving as a diffusing barrier (eg, noble metals Pt, Pd, and Re as well as

refractory metals Ti, W, Ta, and Mo); and (3) highly conductive metal (eg, Au) for bonding. The optical property of mini/micro-LED electrode depends on the exact electrode structure employed. Here, we take two typical electrode materials, transparent ITO and reflective Ag electrode,[42] as examples to show how display performance can be influenced by the optical properties of LED electrode. The LED structures used in our simulation are drawn in Figure 12. When an electric current is applied, the multiple quantum well (MQW) layer could emit light in upward and downward directions. While one-half of the light transmits the transparent ITO and gets lost in the structure of Figure 12A, the Ag electrode in Figure 12B works as a bottom reflector to recycle the downward light, indicating $\alpha_{Ag} = 2$. However, one drawback is that it increases R_{L_LED} from $R_{L\_ITO} = 5.4\%$ to $R_{L\_Ag} = 92.3\%$. For displays, we need to consider human perception when calculating the luminous reflectance:

$$R_{L\_LED} = \frac{\int_{\lambda_1}^{\lambda_2} V(\lambda)S(\lambda)R(\lambda)d\lambda}{\int_{\lambda_1}^{\lambda_2} V(\lambda)S(\lambda)d\lambda}, \tag{10}$$

where $V(\lambda)$ is the photopic human eye sensitivity function, $R(\lambda)$ is the spectral reflectance, and $S(\lambda)$ is the spectrum of the ambient light (CIE Standard Illuminant D65).

Figure 13 depicts the D65 incident light and the simulated reflected light of ITO- and Ag-embedded LEDs. The index matched incident medium is used in our simulations. From the data shown in Figure 13, and using Equation 10, we find $\beta_{Ag} = R_{L\_Ag}/R_{L\_ITO} = 17$.

3.1.3 | CFs and CP

Each CF transmits about 80% of the corresponding emitted RGB LED light but absorbs about two-thirds of the incident ambient (white) light. Figure 14A shows typical RGB LED emission spectra (solid lines) and the
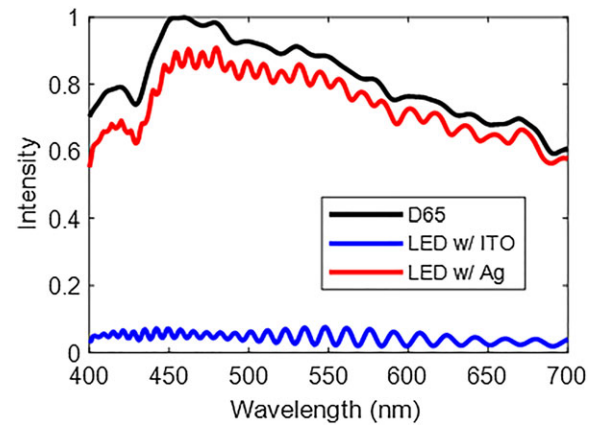
FIGURE 13 Simulated intensity of incident D65 light source and reflected light from a mini/micro–light-emitting diode (LED) with ITO and Ag electrode

transmitted spectra after CFs (dashed lines). In contrast, the incident ambient light passes through the CFs twice due to the reflection of bottom electrode. Thus, in Figure 14B, we plot the D65 incident ambient light (solid line) and the outgoing light after passing through the CFs twice (dashed lines). The obtained effective coefficients are $\alpha_{CF} = 0.75$ and $T_{CF} = 0.184$.

A broadband CP consists of a linear polarizer, a half-wave plate, and a quarter-wave plate. The linear polarizer blocks half of the LED light, corresponding to $\alpha_{CP} = 0.5$. The merit of using a CP is to suppress the internal reflection from the bottom electrode. Because $T_{CP} << R_s$, we set $T_{CP} \sim 0$. However, a serious drawback is that the added CP reduces the panel's flexibility. This is undesirable for flexible displays.

3.1.4 | Surface reflection

As shown in Equation 4, surface reflection plays an important role in external ambient reflection. A normal glass-air surface reflectance is $R_s \approx 4.0\%$, while

FIGURE 12 Mini/micro–light-emitting diode (LED) structures with A, transparent ITO electrode and B, Ag reflective electrode
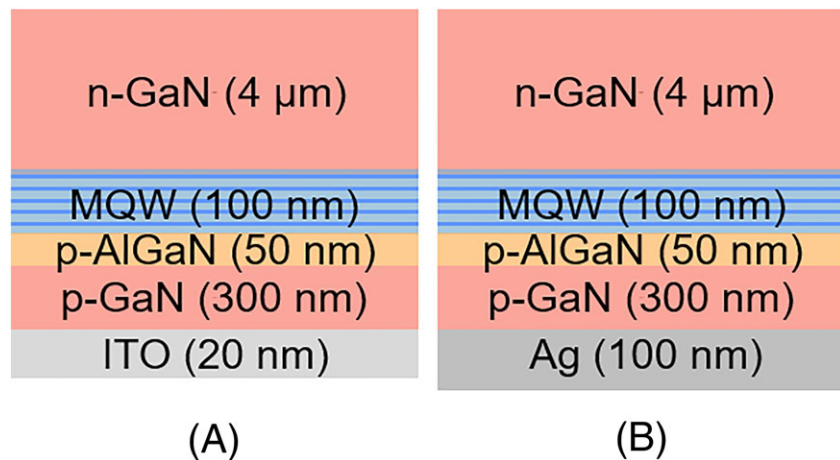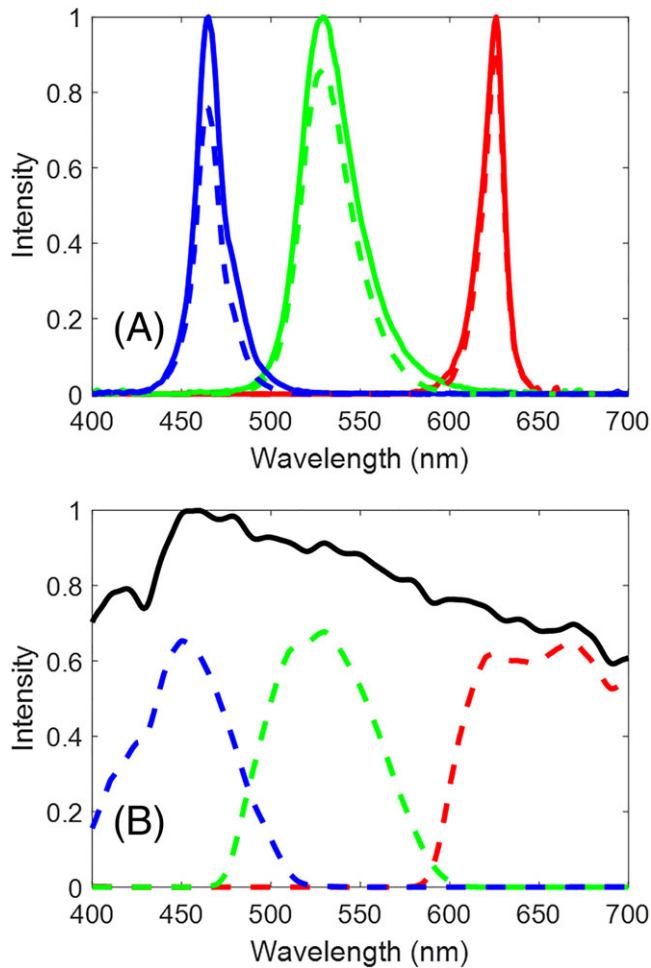
FIGURE 14 A, The RGB emission spectra (solid lines) and the transmittance after passing through a color filter (CF) (dashed lines). B, The D65 white light source (solid line) and the transmittance after passing through a CF twice (dashed lines). The RGB line colors stand for RGB LED/CF colors, respectively

manufacturers have been devoting extensive efforts to lower R_s. DisplayMate has found that Macbook Pro has an impressive $R_s = 0.5\%$ and $R_s = 2\%$ for iPad mini 4 touch panel. While developing antiglare AR solutions for touch panels, several groups, such as TruVue, Dexerials, and NSG, have achieved $R_s < 1\%$. Here, we use the state-of-the-art $R_{s\_AR} = 0.5\%$ for the following analyses.

3.1.5 | Optimal structure

Under a given LED emittance and viewing environment, the ACR is proportional to FoM_o, as Equations 7 and 9 and indicate. For example, if the display luminance in the default design (ITO without CF nor CP) is 1000 cd/m^2, then $FoM_o = 100$ indicates an ACR = 100:1 under 3142 lux overcast daylight. In other words, the optical structure with a higher FoM_o is favorable. To compare

the performance of different designs, we summarize the above-mentioned parameters in Tables 1 and 2.

Figure 15A depicts the calculated FoM_o as a function of AP, which is enlarged in Figure 15B. The highest FoM_o for each AP is obtained by optical structures with Ag electrode (Ag, Ag + CF, and Ag + CP). Ag + CF design is favored for $0.24\% < AP < 1.5\%$, while Ag design and the Ag + CP are preferred for the smaller and the larger AP, respectively. Overall speaking, a high FoM_o (greater than 200) could be maintained with the optimal structures for each AP. That means, if the display luminance in the default ITO design is 500 cd/m^2, the display would well qualify for the requirements of both indoor (ACR = 1000:1 under 314 lux lighting) and outdoor (ACR = 10:1 under 31416 lux strong sunlight) applications.

The influence of R_s on FoM_o can be seen in Figure 15B and 15C. Compared with bare glass surface ($R_s = 4.0\%$ in Figure 15C), AR-coated surface shows an eight times smaller R_s (0.5% in Figure 15B). By plotting FoM_o with eight times scale difference, we find that AR coating helps boost FoM_o by eight times, and the corresponding AP is reduced to one-eighth. This rule can be applied to predict the influence of other surface treatment. If R_s is reduced by n times from 4.0%, similar profile as Figure 15C can be obtained, except for an n-time smaller AP scale and an n-time larger FoM_o scale. After that, the optimal structure for each AP can be obtained.

TABLE 1 Optical parameters in various designs

Structure	α	β	T	R_s
ITO	1	1	1	R_{s_AR}
ITO + CF	α_{CF}	1	T_{CF}	R_{s_AR}
ITO + CP	α_{CP}	1	T_{CP}	R_{s_AR}
Ag	α_{Ag}	β_{Ag}	1	R_{s_AR}
Ag + CF	$\alpha_{Ag} \cdot \alpha_{CF}$	β_{Ag}	T_{CF}	R_{s_AR}
Ag + CP	$\alpha_{Ag} \cdot \alpha_{CP}$	β_{Ag}	T_{CP}	R_{s_AR}

Abbreviations: CF, color filter; CP, circular polarizer.

TABLE 2 Parameters used for simulation

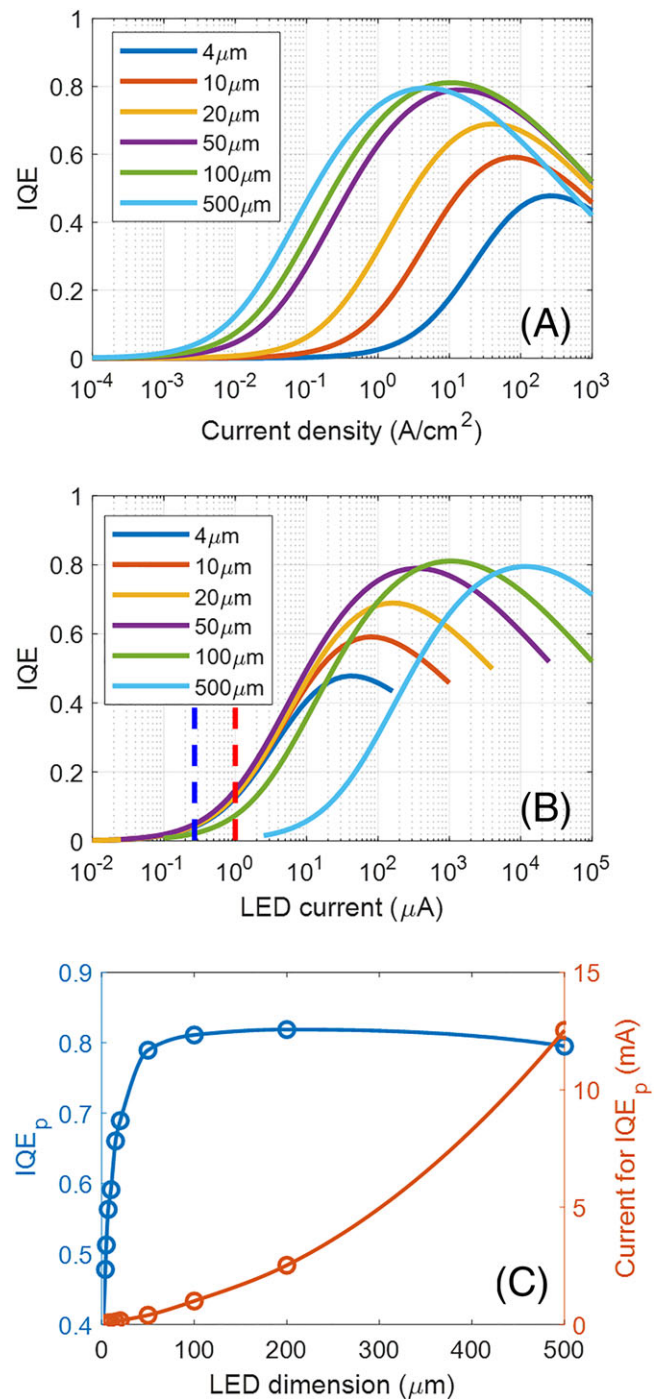|		
Ag	α_{Ag}	2
	β_{Ag}	17
CF	α_{CF}	0.75
	T_{CF}	0.184
CP	α_{CP}	0.5
	T_{CP}	Approximately 0
AR	R_{s_AR}	0.50%

Abbreviations: AR, antireflection; CF, color filter; CP, circular polarizer.
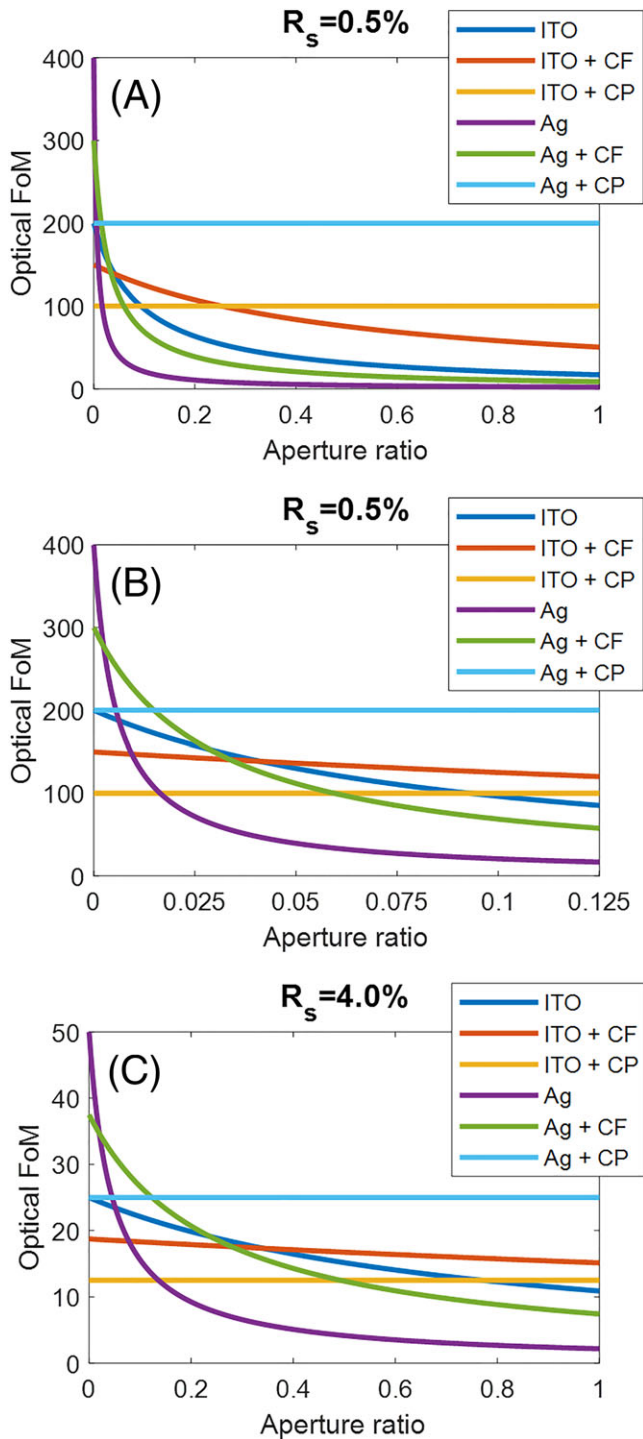
FIGURE 15 *FoM$_o$* of different optical structures as a function of *AP*: A, full-scale plot for $R_s = 0.5\%$; B, enlarged plot for $R_s = 0.5\%$; C, full-scale plot for $R_s = 4.0\%$

FIGURE 16 A, Current density-dependent internal quantum efficiency (IQE) and B, light-emitting diode (LED) current-dependent IQE for different LED dimensions. (c) *IQE$_p$* and the corresponding current for different LED dimensions

3.2 | Electrical driving IQE

Due to the surface defect-generated sidewall effect,[43] impaired quantum efficiency on small-chip mini/micro-LEDs has been observed. Several groups have reported current density-dependent IQE with the trend shown in Figure 16A.[44–46]

As the current density (or current as Figure 16B depicts) increases, IQE increases to a peak value (*IQE$_p$*) and then declines. Details depend on the chip size. As the blue line shows in Figure 16C, *IQE$_p$* increases drastically as *s* (defined in Equation 5) increases from 4 to 50 μm and then saturates in the 50 to 500 μm region.

Unfortunately, the LEDs cannot be always driven at the sweet spot if analog driving with 100% duty cycle is adopted. Taking a 65-inch 4K2K TV as an example, the panel area is $A_{panel} = 1.16$ m^2. Assuming display luminance $L_{on} = 1000$ cd/m^2 and luminous efficiency $\eta_L = 200$ lm/W,[47] the electric power of the panel is $P_{panel} = 18.2$ W, as calculated from

$$\pi \cdot L_{on} \cdot A_{panel} = \eta_L \cdot P_{panel}. \qquad (11)$$

Applying a typical forward voltage $V_f = 3$ V, the current flowing through the LEDs in the whole panel is

$$I_{panel} = P_{panel}/V_f = 6.1A. \qquad (12)$$

For the 4K2K resolution, the number of RGB LEDs (N_{LED}) and the single-LED current (I_{LED}) are

$$N_{LED} = 3840 \times 2160 \times 3; \qquad (13)$$

$$I_{LED} = I_{panel}/N_{LED} = 0.24\mu A. \qquad (14)$$

Figure 16B shows the relationship between IQE and I_{LED}. To be noticed, the IQE is relatively low at such a small current (as the blue dashed lines mark), resulting in low η_L and inadequate luminance. Therefore, a higher $I_{LED} \sim 1$ μA (red dashed lines) may be required to produce $L_{on} = 1000$ cd/m^2. Although the above-mentioned parameters may vary in different panels, the calculated I_{LED} should be in the same order, which is about 100× lower than the I_{LED} for optimal IQE (50-1000 μA for $s \leq 50$ μm). As a result, the energy efficiency is low in analog driving scheme. In order to boost η_L, pulse width modulation (PWM) with low duty cycle can be utilized so that the

LEDs can be always driven at the desired IQE_p, corresponding to the η_L in digital driving scheme. Therefore, it is reasonable to use LED size-dependent IQE_p as a metric to evaluate power efficiency. Here, we define an electrical figure-of-merit (FoM_e) as

$$FoM_e = IQE_p, \qquad (15)$$

which is plotted as the blue line in Figure 16C.

3.3 | Optimization strategy

Until now, we have discussed the AP-dependent FoM_o and the LED chip size-dependent FoM_e. Let us return to the basic questions of designing a mini/micro-LED emissive display: what are the optimal LED chip size and optical structure? In order to answer these questions, we need to consider both optical and electrical performances together. Thus, let us define an optical-electrical figure-of-merit (FoM_{oe}) as

$$FoM_{oe} = FoM_o \cdot FoM_e. \qquad (16)$$

The FoM_{oe} indicates how high an ACR can be obtained by the user with a given power consumption.

Figure 17 shows the FoM_{oe} as a function of s for different pixel pitch length. We only plot the structures with Ag electrode because Figure 15 shows that it has better optical performance. As demonstrated in Figure 17, a peak FoM_{oe} exists in the small s region for the Ag (blue lines) and Ag + CF (red lines) designs. This is because a small AP helps reduce internal reflection. In contrast, for the Ag + CP design, CP helps suppress internal
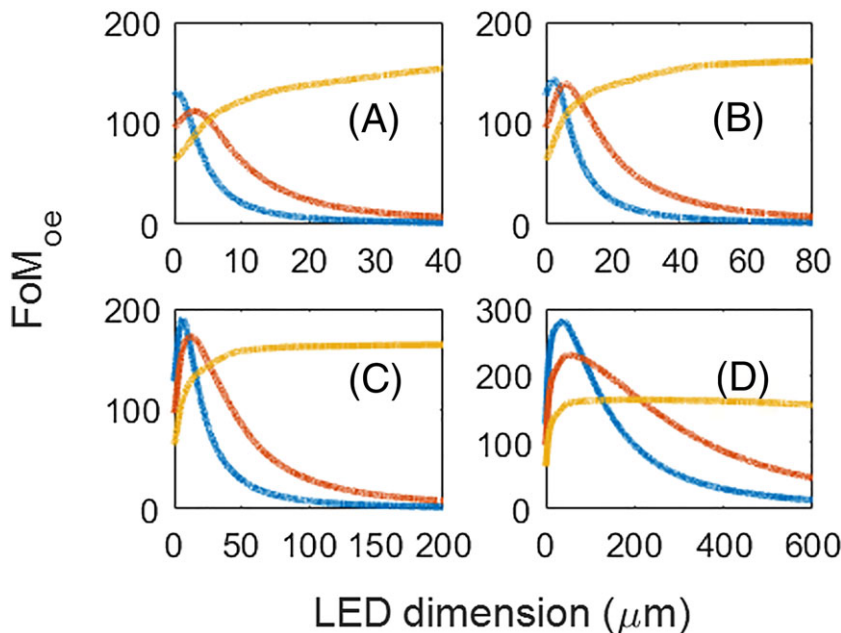
FIGURE 17 Simulated FoM_{oe} as a function of s for different p: A, $p = 73$ μm for $d = 25$ cm (smartphone); B, $p = 145$ μm for $d = 50$ cm (gaming monitors); C, $p = 375$ μm for 65-inch 4K TV; D, $p = 3$ mm for 12.3-m-wide 4K scope display for movie theaters. The pitch length p is calculated by viewing distance d and 1-arcminute human eye acuity. The blue, red, and yellow lines stand for the Ag, Ag + CF, and Ag + CP structure, respectively

reflection so that R_L and FoM_o do not change with s. Therefore, FoM_{oe} increases with s and then saturates, showing the same trend as FoM_e (the yellow lines in Figure 17 and the blue line in Figure 16C). Please note that these results are calculated based on the parameters listed in Table 2. Other electrode materials, CFs, surface treatment, and electrical properties may change the line shape in Figure 17. Nevertheless, our analyses remain valid, and the trend for each design should be similar.

From the comparison in Figure 17, we can see that the optimal optical structure depends on the pixel pitch. For personal flat panel displays (Figure 17A and 17B), Ag + CP is preferred since it provides comparable or better performance. In the meantime, the highest FoM_{oe} appears at a much larger s than that of Ag and Ag + CF designs, and the higher operating IQE implying less nonradiative heating issue. Differently, for public displays with large pitch length (Figure 17C and 17D), Ag and Ag + CF present a higher peak FoM_{oe}, and the corresponding s is within the fabrication range. For example, for a 3-mm pitch cinema display, its peak FoM_{oe} occurs at $s = 39$ μm with the Ag design, as the blue curve in Figure 17C shows. The small die size yet without the need of a large-area CP is not only cost-effective but also advantageous for flexible displays.

4 | CONCLUSION

We have described two types of mini/micro-LED displays: (1) As a LCD backlight, the zoned mini-LED enables local dimming, which helps suppress the halo effect and the clipping effect. Through numerical simulation and subjective experiments, we find that halo effect can be suppressed to an unnoticeable level, depending on the LCD's CR and local dimming zone numbers. For example, around 3000 and 200 local dimming zones are, respectively, required for an FFS LCD with CR ≈ 2000:1 and an MVA LCD panel with CR = 5000:1 for a 6.4-inch smartphone placed at 25 cm. These results can also be extended to large-size panels according to the viewing distance. A well-confined light of each LED or each local dimming zone could reduce the interzone crosstalk and clipping effect but may result in severe uniformity issue. (2) Similar to OLED displays, RGB mini/micro-LED emissive displays exhibit an excellent dark state but the strong internal reflection may give rise to compromised ACR. Besides, micro-LEDs faces low IQE problem on small-size chips. We have also analyzed the influence of each optical component and suggested the optimal LED chip-size considering both ACR and power efficiency. Our work would help optimize device and system

designs. Widespread application of mini/micro-LED for HDR displays is around the corner.

ORCID

*Shin-Tson Wu* [ID] https://orcid.org/0000-0002-0943-0440

REFERENCES

1. Schadt M. Milestone in the history of field-effect liquid crystal displays and materials. Jpn J Appl Phys. 2009;48:03B001.

2. Tang CW, Vanslyke SA. Organic electroluminescent diodes. Appl Phys Lett. 1987;51:913–915.

3. Chen H-W, Lee J-H, Lin B-Y, Chen S, Wu S-T. Liquid crystal display and organic light-emitting diode display: present status and future perspectives. Light: Sci & Appl. 2018;7:17168.

4. Tan G, Zhu R, Tsai Y, et al. High ambient contrast ratio OLED and QLED without a circular polarizer. J Phys D Appl Phys. 2016;49:315101.

5. Zhu R, Luo Z, Chen H, Dong Y, Wu S-T. Realizing Rec. 2020 color gamut with quantum dot displays. Opt Express. 2015;23(18):23680–23693.

6. Peng F, Chen H, Gou F, et al. Analytical equation for the motion picture response time of display devices. J Appl Phys. 2017;121(2):023108.

7. Féry C, Racine B, Vaufrey D, Doyeux H, Cinà S. Physical mechanism responsible for the stretched exponential decay behavior of aging organic light-emitting diodes. Appl Phys Lett. 2005;87(21):213502.

8. Murawski C, Leo K, Gather MC. Efficiency roll-off in organic light-emitting diodes. Adv Mater. 2013;25:6801–6827.

9. Daly S, Kunkel T, Sun X, Farrell S, Crum P. Viewer preferences for shadow, diffuse, specular, and emissive luminance limits of high dynamic range displays. SID Intl Symp Dig Tech Pap. 2013;44(1):563–566.

10. Park S, Xiong Y, Kim R, et al. Printed assemblies of inorganic light-emitting diodes for deformable and semitransparent displays. Science. 2009;325(5943):977–981.

11. Jiang HX, Lin JY. Nitride micro-LEDs and beyond—a decade progress review. Opt Express. 2013;21(S3):A475–A484.

12. Templier F. GaN-based emissive microdisplays: a very promising technology for compact, ultra-high brightness display systems. J Soc Inf Display. 2017;24(11):669–675.

13. Tan G, Huang Y, Li M-C, Lee S-L, Wu S-T. High dynamic range liquid crystal displays with a mini-LED backlight. Opt Express. 2018;26(13):16572–16584.

14. Chen H, Tan G, Wu S-T. Ambient contrast ratio of LCDs and OLED displays. Opt Express. 2017;25(26):33643–33656.

15. Shirai T, Shimizukawa S, Shiga T, Mikoshiba S, Käläntär K. RGB-LED backlights for LCD-TVs with 0D, 1D, and 2D adaptive dimming. SID Intl Symp Dig Tech Pap. 2006;37(1):1520–1523.

16. Hulze HG, de Greef P. Power savings by local dimming on a LCD panel with side lit backlight. SID Intl Symp Dig Tech Pap. 2009;40(1):749–752.

17. Bonar JR, Valentine GJ, Gong Z, Small J, Gorton S. High-brightness low-power consumption microLED arrays. Proc SPIE. 2016;9768:97680Y.

18. Seetzen H, Whitehead LA, Ward G. A high dynamic range display using low and high resolution modulators. SID Intl Symp Dig Tech Pap. 2003;34(1):1450–1453.

19. Seetzen H, Heidrich W, Stuerzlinger W, et al. High dynamic range display systems. ACM Trans Graph. 2004;23(3):760–768.

20. de Greef P, Hulze HG. Adaptive dimming and boosting backlight for LCD-TV systems. SID Intl Symp Dig Tech Pap. 2007;38(1):1332–1335.

21. Lin F, Huang Y, Liao L, et al. Dynamic backlight gamma on high dynamic range LCD TVs. J Disp Technol. 2008;4(2):139–146.

22. Chen H, Ha TH, Sung JH, Kim HR, Han BH. Evaluation of LCD local-dimming-backlight system. J Soc Inf Display. 2010;18(1):57–65.

23. Kim S, An J-Y, Hong J-J, Lee TW, Kim CG, Song W-J. How to reduce light leakage and clipping in local-dimming liquid-crystal displays. J Opt Soc Am A. 2009;17(12):1051–1057.

24. Burini N, Nadernejad E, Korhonen J, Forchhammer S, Wu X. Modeling power-constrained optimal backlight dimming for color displays. J Disp Technol. 2013;9(8):656–665.

25. Deng Z, Zheng B, Zheng J, et al. High dynamic range incell LCD with excellent performance. SID Intl Symp Dig Tech Pap. 2018;49(1):996–998.

26. Day J, Li J, Lie DYC, Bradford C, Lin JY, Jiang HX. III-Nitride full-scale high-resolution microdisplays. Appl Phys Lett. 2011;99:031116.

27. Henry W, Percival C. ILED displays: next generation display technology. SID Intl Symp Dig Tech Pap. 2016;47:747–750.

28. Chen H, He J, Wu S-T. Recent advances on quantum-dot-enhanced liquid-crystal displays. IEEE J Sel Top Quantum Electron. 2017;23(5):1–11. 1900611

29. He J, Chen H, Chen H, Wang Y, Wu S-T, Dong Y. Hybrid downconverters with green perovskite-polymer composite films for wide color gamut displays. Opt Express. 2017;25(11):12915–12925.

30. Lin H-Y, Sher C-W, Hsieh D-H, et al. Optical cross-talk reduction in a quantum- display by a lithographic-fabricated photoresist mold. Photonics Res. 2017;5(5):411–416.

31. Chen G-S, Wei B-Y, Lee C-T, Lee H-Y. Monolithic red/green/blue micro-LEDs with HBR and DBR structures. IEEE Photonics Technol Lett. 2018;30(3):262–265.

32. Beckers A, Fahle D, Mauder C, Kruecken T, Boyd AR, Heuken M. Enabling the next era of display technologies by micro LED MOCVD processing. SID Intl Symp Dig Tech Pap. 2018;49(4):601–603.

33. Bower CA, Meitl MA, Raymond B, et al. Emissive displays with transfer-printed assemblies of 8 μm × 15 μm inorganic light-emitting diodes. Photonics Res. 2017;5(2):A23–A29.

34. Wu T, Sher C, Lin Y, et al. Mini-LED and micro-LED: Promising candidates for the next generation display technology. Appl Sci. 2018;8(9):1557.

35. Chen H, Tan G, Li M-C, Lee S-L, Wu S-T. Depolarization effect in liquid crystal displays. Opt Express. 2017;25(10):11315–11328.

36. Sun C, Chien W, Moreno I, et al. Calculating model of light transmission efficiency of diffusers attached to a lighting cavity. Opt Express. 2010;18(6):6137–6148.

37. Woodgate GJ, Harrold J, Limited O, Park H, Heyford U, Ox O. Micro-optical systems for micro-LED displays. SID Intl Symp Dig Tech Pap. 2018;49(1):1559–1562.

38. Paranjpe A, Montgomery J, Lee SM, Morath C. Micro-LED displays: key manufacturing challenges and solutions. SID Intl Symp Dig Tech Pap. 2018;49(1):597–600.

39. Chaji R, Fathi E, Zamani A. Low-cost micro-LED displays for all applications. SID Intl Symp Dig Tech Pap. 2017;48(1):264–267.

40. Schubert EF. Light-emitting diodesTroy: E. Fred Schubert; 2018.

41. Wong MS, Hwang D, Alhassan AI, et al. High efficiency of III-nitride micro-light-emitting diodes by sidewall passivation using atomic layer deposition. Opt Express. 2018;26(16):21324–21331.

42. Liu Z, Wang K, Luo X, Liu S. Precise optical modeling of blue light-emitting diodes by Monte Carlo ray-tracing. Opt Express. 2010;18(9):9398–9412.

43. Tian P, McKendry JJD, Gong Z, et al. Size-dependent efficiency and efficiency droop of blue InGaN micro-light emitting diodes. Appl Phys Lett. 2012;101(23):231110.

44. Olivier F, Daami A, Licitra C, Templier F. Shockley-Read-Hall and Auger non-radiative recombination in GaN based LEDs: a size effect study. Appl Phys Lett. 2017;111(2):022104.

45. Bourim EM, Han JI. Size effect on negative capacitance at forward bias in InGaN/GaN multiple quantum well-based blue LED. Electron Mater Lett. 2016;12(1):67–75.

46. Konoplev SS, Bulashevich KA, Karpov SY. From large-size to micro-LEDs: scaling trends revealed by modeling. Phys Status Solidi Appl Mater Sci. 2018;215(10):1700508.

47. Sadeghi S, Kumar BG, Melikov R, Aria MM, Jalali HB, Nizamoglu S. Quantum dot white LEDs with high luminous efficiency. Optica. 2018;5(7):793–802.
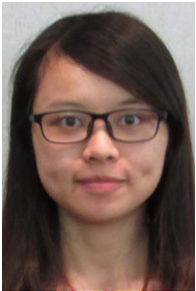
AUTHOR BIOGRAPHIES

Yuge Huang received her BS degree in physics from Nanjing University, China, in 2015 and is currently working toward the PhD degree at College of Optics and Photonics, University of Central Florida, Orlando, FL, USA. Her research focuses on mini-LED backlit LCDs and fast-response liquid crystal devices for augmented reality and virtual reality displays. She received SID Metro Detroit Academic Award in 2018.
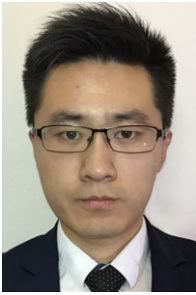
Guanjun Tan received a BS degree in Physics from University of Science and Technology of China in 2014 and is currently working toward the PhD degree at the College of Optics and Photonics, University of Central Florida. His current research interests include head-mounted displays, organic LED displays, and novel liquid crystal displays.

Fangwang Gou received her BS degree from University of Electronic and Science and Technology of China in 2012 and MS degree from Peking University, China, in 2015. Currently, she is working toward the PhD degree at College of Optics and Photonics, University of Central Florida, USA. Her current research interests include optical devices for liquid crystal displays, augmented reality and virtual reality, and micro-LEDs.

Ming-Chun Li received his BS degree in Electronic Engineering, Feng Chia University, Taiwan, in 2000 and MS degree from National Sun Yat-Sen University, Taiwan, in 2005. Currently, he is a manager at AU Optronics, in charge of LCD cell material and process technology development.

Seok-Lyul Lee received his BS degree in Electronic Communication Engineering, Kwangwoon University, Korea, in 1992 and MS degree from Chonbuk National University, Korea, in 2010. Currently, he is a principal engineer and fellow at AU Optronics. He is one of the key inventors of fringe-field switching (FFS) liquid crystal display. He contributed to development and commercialization of mobile, tablet, and monitor TFT-LCD products using the FFS mode. He received SID Special Recognition Award in 2012 and SID Fellow Award in 2018.

Shin-Tson Wu is Pegasus professor at College of Optics and Photonics, University of Central Florida. He is among the first six inductees of the Florida Inventors Hall of Fame (2014) and a Charter Fellow of the National Academy of Inventors (2012). He is a fellow of the IEEE, OSA, SID, and SPIE, and an honorary professor of National Chiao Tung University (2018) and of Nanjing University (2013). He is the recipient of 2014 OSA Esther Hoffman Beller Medal, 2011 SID Slottow-Owaki Prize, 2010 OSA Joseph Fraunhofer Award, 2008 SPIE G. G. Stokes Award, and 2008 SID Jan Rajchman Prize. Presently, he is serving as SID honors and awards committee chair.